

Phase Transition Generated Cosmological Magnetic Field at Large Scales

Tina Kahniashvili^{a,b*}, Alexander G. Tevzadze^{b†}, Bharat Ratra^{c‡}

^aMcWilliams Center for Cosmology and Department of Physics, Carnegie Mellon University, 5000 Forbes Ave, Pittsburgh, PA 15213, USA

^bNational Abastumani Astrophysical Observatory, Ilia Chavchavadze State University, 2A Kazbegi Ave, Tbilisi, GE-0160, Georgia

^cDepartment of Physics, Kansas State University, 116 Cardwell Hall, Manhattan, KS 66506

We constrain a primordial magnetic field (PMF) generated during a phase transitions (PT) using big bang nucleosynthesis (BBN) bounds on the relativistic energy density. The amplitude of the PMF at large scales is determined by the spectral shape of the PMF spectrum outside its maximal correlation length scale. Even if the amplitude of the PMF at 1 Mpc is small, PT generated PMFs can leave observable signatures in the potentially detectable relic gravitational wave background if a large enough fraction ($1 - 10\%$) of the thermal energy is converted into the PMF.

1. Introduction

A cosmological seed PMF (generated during or prior to the radiation-dominated epoch) has been proposed to explain the existence of observed $\sim 10^{-6} - 10^{-5}$ Gauss (G) magnetic fields in galaxies and clusters [1, 2]. To preserve approximate spatial isotropy a PMF has to be small and hence can be treated as a first order term in perturbation theory. In the standard cosmological model [3] the energy density parameter of a PMF, $\Omega_B = \rho_B / \rho_{\text{cr}}$, is significantly less than unity. Also, a PMF must be smaller than those observed in galaxies (10^{-5} G), so $\Omega_B h_0^2 < 10^{-4}$ where h_0 is the Hubble constant in units of $100 \text{ km s}^{-1} \text{ Mpc}^{-1}$. Since the PMF energy density contributes to the radiation field, the BBN bound implies $\Omega_B h_0^2 \leq 2.4 \times 10^{-6}$. The ratio of ρ_B and the energy density of radiation ρ_{rad} is constant during cosmological evolution, if the PMF is not damped by an MHD (or other) process and so stays frozen to the plasma. Direct measurement of a cosmological MF is based on the Faraday rotation effect. A potential extension of this method, based on the rotation of the cosmic microwave background (CMB) polarization plane, appears promising [4, 5]. In addition, a PMF leaves imprints on the CMB temperature and polarization anisotropies (for a review see Ref. [6]).

*tinatin@phys.ksu.edu

†aleko@tevza.org

‡ratra@phys.ksu.edu

In this paper we consider cosmological PMFs generated by causal processes during phase transitions (PTs) such as the electroweak (EW) and QCD PTs [7]. The main parameters of interest are the temperature T_* and the number of relativistic degrees of freedom g_* when the PMF is generated. We only use fundamental physical laws, such as conservation of energy and how the magnetic field interacts with the cosmological plasma through MHD turbulence, and do not make any assumption about the physical process leading to PMF generation. We discuss cosmological signatures of such a PMF, including the effects on the CMB temperature and polarization anisotropies and the production of gravitational waves (GWs). We employ natural units with $\hbar = 1 = c$ and gaussian units for electromagnetic quantities.

2. Magnetic Field Spectrum

The maximal correlation length l_{\max} at generation of a causally generated PMF cannot exceed the Hubble radius H_*^{-1} then, so $\gamma = l_{\max}/H_*^{-1} \leq 1$, where γ can be associated with the number of PMF bubbles within the Hubble radius, $N \propto \gamma^3$. The comoving length (measured today) corresponding to the Hubble radius is inversely proportional to the temperature T_* ,

$$\lambda_H = 5.8 \times 10^{-10} \text{ Mpc} \left(\frac{100 \text{ GeV}}{T_*} \right) \left(\frac{100}{g_*} \right)^{1/6}, \quad (1)$$

and is equal to 0.5 pc for the QCDPT (with $g_* = 15$ and $T_* = 0.15 \text{ GeV}$) and $6 \times 10^{-4} \text{ pc}$ for the EWPT (with $g_* = 100$ and $T_* = 100 \text{ GeV}$), and the comoving PMF correlation length $\xi_{\max} \leq \lambda_H$.

If generated prior to BBN, the maximal value of the PMF energy density must satisfy the BBN bound, i.e. the total energy density of the PMF at nucleosynthesis, $\rho_B(a_N)$, should not exceed 10% of the radiation energy density then, $\rho_{\text{rad}}(a_N)$. Since the ratio ρ_B/ρ_{rad} is constant, the maximal comoving value of the effective PMF $B^{(\text{eff})} = \sqrt{8\pi\rho_B} = 8.4 \times 10^{-7} (100/g_*)^{1/6} \text{ G}$, if no PMF damping occurs before BBN. Even if the PMF energy is converted to another field contributing to the radiation (for example, GWs [8, 9]), there is only $\rho_B(a_*)$ magnetic energy available. The next issue is to determine how this energy is distributed at different wavelengths, and the comoving PMF at a given comoving length scale λ . Of course, for a scale-invariant [10] or homogeneous PMF the limit remains the same at any scale. Note that the maximal value of the PMF (from the BBN bound) is independent of the temperature at generation T_* , and depends only very weakly on the number of relativistic degrees of freedom then.

ρ_B can be viewed as the magnetic energy density injected into the cosmological plasma at the comoving length scale λ_0 , the size of the largest magnetic eddy. After generation, PMF evolution (during the PT) depends crucially on the length scale under consideration. If the relevant time scales are shorter than H_*^{-1} we can neglect the expansion of the Universe. In this case, we must distinguish three sub-Hubble-radius regimes: $k_H < k < k_0$ (where $k_H = 2\pi/\lambda_H$ and $k_0 = 2\pi/\lambda_0$; the large scale decay regime), $k_0 < k < k_D$ with $k_D = 2\pi/\lambda_D$ the damping wavenumber scale related to plasma properties (the turbulence regime), and $k > k_D$ (the viscous damping regime). The interaction of the PMF with the plasma, and as a consequence the dynamics of the PMF, is sensitive to the presence of magnetic helicity (see Refs. [11] for magnetic helicity generation mechanisms).

The magnetic energy $E_M(k, t)$ and helicity $H_M(k, t)$ density power spectra are related to the magnetic energy and helicity densities through $\mathcal{E}_M(t) = \int_0^\infty dk E_M(k, t)$ and $\mathcal{H}_M(t) = \int_0^\infty dk H_M(k, t)$. The magnetic correlation length $\xi_M(t) = [\int_0^\infty dk k^{-1} E_M(k, t)] / \mathcal{E}_M(t)$ corresponds to the largest eddy length scale. All configurations of the MF must satisfy the “realizability condition” [12]: $|\mathcal{H}_M(t)| \leq 2\xi_M(t)\mathcal{E}_M(t)$. Also, the velocity energy density spectrum $E_K(k, t)$ is related to the kinetic energy of turbulent motions through $\mathcal{E}_K(t) = \int_0^\infty dk E_K(k, t)$.

2.1. Magnetic Field Spatial Structure

We first consider the non-helical case. For large enough Reynolds number the magnetic energy is re-distributed by a Kolmogoroff turbulence direct cascade. From the analogy between the Kolmogoroff laws for hydrodynamic and magnetic turbulence, the magnetic energy dissipation comoving rate per unit enthalpy is $\varepsilon_M \simeq (2/3)^{3/2} k_0 v_A^3$, with $v_A = \sqrt{1.5\rho_B/\rho_{\text{rad}}}$ being the effective Alfvén velocity corresponding to the total fluid-injected PMF energy, i.e. $\varepsilon_M = k_0(\rho_B/\rho_{\text{rad}})^{3/2}$. In the absence of PMF damping at $k = k_0$, for Kolmogoroff turbulence, $E_M(k) = C_M \rho_B k_0^{-1} \bar{k}^{-5/3}$ when $k_0 < k < k_D$, where C_M is a constant of order unity and $\bar{k} = k/k_0$. At large scales when $k < k_0$ we model the PMF energy spectrum by a power law, $E(k) \propto k^\alpha$. Requiring continuity of the PMF spectrum at $k = k_0$, $E(k) = C_M \rho_B k_0^{-1} \bar{k}^\alpha$ for $k < k_0$. It is natural to assume that the MF energy injection scale λ_0 is the same as the maximal correlation length of the PMF, i.e. $\lambda_0 \simeq l_{\text{max}} a_0 / a_\star$.

The largest scale MF energy density spectral index α has been much discussed. Hogan [13] requires causality of the field and argues that the PMF energy density spectrum must be white noise for scales larger than the causal horizon, λ_0 . This corresponds to $\alpha = 2$. Durrer and Caprini [14] claim that this violates the divergence-free PMF requirement and instead demand $\alpha = 4$. Both of these spectra, $\alpha = 2$ (Saffman) and $\alpha = 4$ (Batchelor),⁴ are well known in the turbulence literature and, as discussed in Ref. [15], their realization depends on initial conditions. Another possibility is Kazantsev’s $\alpha = 3/2$ value, which can be rapidly achieved during the turbulence decay process discussed in Refs. [16]. To keep the analysis as general as possible, we keep α arbitrary as much as possible.

Requiring $E_M \leq \rho_B$ we obtain $C_M \leq 1.5(\alpha + 1)/(3\alpha + 5)$. With $\rho_B \leq 0.1\rho_{\text{rad}}$ and neglecting the contribution to the energy density from scales smaller than the damping scale λ_D , for the maximal allowed value of C_M , we have $C_M \rho_B \leq 2.81 \times 10^{-14} C_{M,\text{max}} (100/g_\star)^{1/3} \text{ G}^2$, and the magnetic energy spectrum

$$E_M(\bar{k}) \leq 0.22 C_{M,\text{max}} \left(\frac{100 \text{ GeV}}{T_\star} \right) \left(\frac{100}{g_\star} \right)^{5/6} \gamma \frac{(10^{-9} \text{ G})^2}{\text{pc}^{-1}} \left\{ \begin{array}{ll} \bar{k}^\alpha & \text{if } \bar{k} < 1 \\ \bar{k}^{-5/3} & \text{if } \bar{k} > 1 \end{array} \right\}. \quad (2)$$

Note the damping wavenumber k_D is determined by the Reynolds number $\text{Re} \gg 1$ of the fluid during the PT, as $k_D = k_0 \text{Re}^{3/4}$.

Defining B_λ as a smoothed PMF over a sphere of radius λ ($\lambda > \lambda_0$) we have for the MF energy density on scales larger than the maximal correlation length, $\mathcal{E}_M^{\text{LS}} = \int_0^{k_0} dk E_M(\bar{k}) = B_\lambda^2 (k_0 \lambda)^{\alpha+1} / [8\pi \Gamma(0.5\alpha + 1.5)]$ where Γ is the Euler Gamma function, [17]. This leads to the upper bound $B_\lambda \propto \lambda^{-(\alpha+1)/2}$ shown in Fig. 1. The PMF limits shown in Fig. 1 does not account for the evolution and damping of the PMF during the expansion of the

⁴ $E \sim k^4$ is sometimes called the von Kármán spectrum.

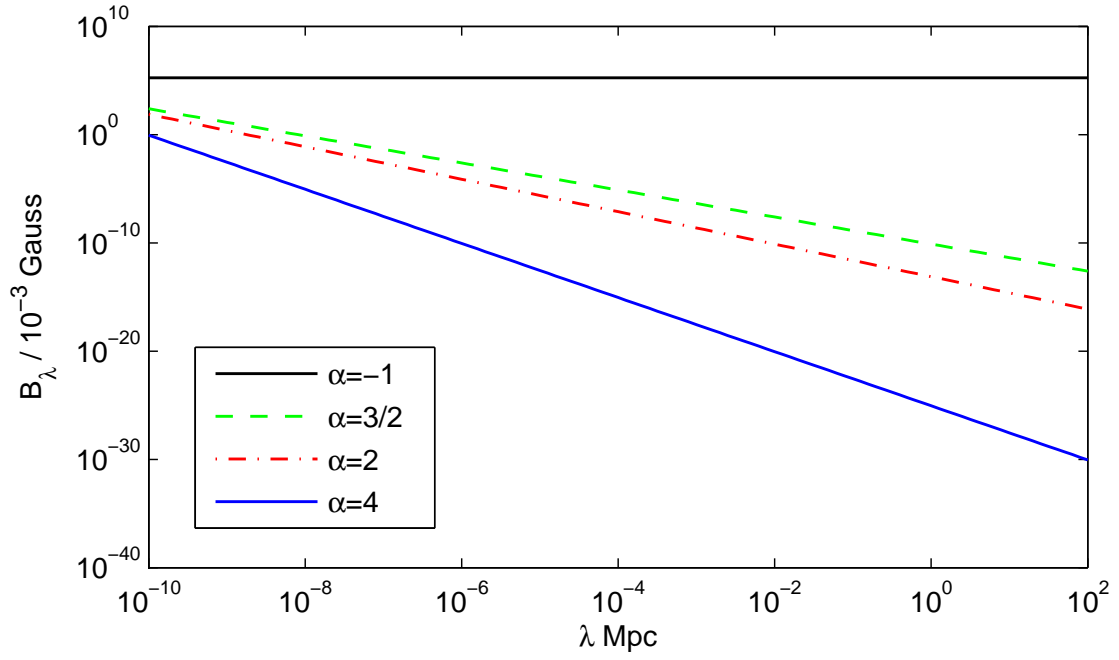


Figure 1. The maximal allowed value B_λ for a PMF generated during the EWPT with $T_\star = 100 \text{ GeV}$, $g_\star = 100$, and $\gamma = 0.01$.

Universe, addressing only the spatial structure of the PMF at large scales constrained by the BBN bound on the relativistic component energy density. Based on dimensional analysis we address the time evolution of the PMF in the next subsection, with more precise computations presented in Ref. [18].

2.2. Magnetic Field Temporal Characteristics

The PMF spectrum is characterized not only by its spatial distribution, but also by its characteristic times: i) the largest size eddy turn-over time $\tau_0 \simeq l_0/v_A$, which can also be used to determine the minimal duration of the source needed to justify use of the stationary turbulence approximation [19];⁵ and, ii) the turbulence cascade time-scale τ_{dc} and the large-scale turbulence decay time τ_{ls} . If the source duration time is short compared to the Hubble time H_\star^{-1} we can neglect the expansion of the Universe. For the EWPT ($\gamma \simeq 0.01$), and for reasonable moderate values of the Alfvén velocity ($v_A \leq 0.3$), the maximal size magnetic eddy turn-over time scale $\tau_0 \simeq \gamma H_\star^{-1}/v_A$ is significantly shorter than the Hubble time H_\star^{-1} . Also, τ_{dc} is determined by the dissipation rate ε_M . To proceed we specify the time decorrelation function $f(\eta(k), \tau)$, as $f_{dc}[\eta(k), \tau] = \exp[-\pi\eta^2(k)\tau^2/4]$ for $k_0 < k < k_D$ [21], where $\eta(k) = \varepsilon^{1/3}k^{2/3}/\sqrt{2\pi}$. For non-helical turbulence, by considering the largest size magnetic eddy decorrelation, $\tau_{dc} \simeq 0.5\tau_0$, thus the direct cascade time scale is much shorter than the Hubble time, and the assumption made above to neglect the energy density for $\lambda < \lambda_0$ is justified, as is the assumption to neglect the expansion of the Universe during the direct cascade.

The other characteristic time is related to the decay of large-scale turbulence. Specific to this process is that there is no magnetic or hydrodynamic turbulence production source and free decay occurs. In this case here we may adopt the grid turbulence decay law $k(t) \propto t^{-1.3}$ (see e.g. [22]). This can be motivated by noting that the correlation length and the Hubble radius set natural length scales which are the analogue of the grid size in laboratory turbulence. Assuming that \bar{k} is time independent during the decay and $\mathcal{E}_M(t) \propto t^{-2}$, we get $E_M(\bar{k}, t) \propto \bar{k}^\alpha t^{-0.7}$ when $\bar{k} < 1$. Figure 2 shows the spatial and temporal surface of freely decaying turbulence at large scales ignoring MHD dynamo effects. The time scale is normalized to the largest size magnetic eddy turn-over time τ_0 . For scales k in the range $k_0 < k < k_D$, temporal decorrelation occurs in a time interval much shorter than the time scale related to the free decay of turbulence. Thus the free decay timescale is important only at large scales. The grid turbulence analogy implies that the PMF spectral energy density is decreased by several orders of magnitudes within a period of $10\tau_0$ (well within the EWPT Hubble time H_\star^{-1}), indicating that the expansion of the Universe can be neglected. After free decay reduces the MF power, the PMF on scales $k \ll k_0$ can be treated as a MF that is unaffected by turbulence. Of course, when considering realistic cosmological turbulence, in contrast to the laboratory turbulence case, the evolution of the fluid viscosity must be taken into account, which can change the PMF correlation length and energy density scaling laws shown here, see also Ref. [23] for a different model of free-decaying MHD turbulence. We also argue [18] that free

⁵Since, for the developed turbulence case, the magnetic energy proper dissipation rate per unit enthalpy, $\bar{\varepsilon}_M = \varepsilon_M a_0/a_\star$, must be approximately equal to the mean energy input rate per unit enthalpy of the source, i.e. the turbulence cascade time scale $\tau_{dc} \simeq 2\pi\bar{\varepsilon}_M^{-1}(\rho_B/w_{rad}) \simeq \tau_0$ where w_{rad} is the radiation enthalpy [20].

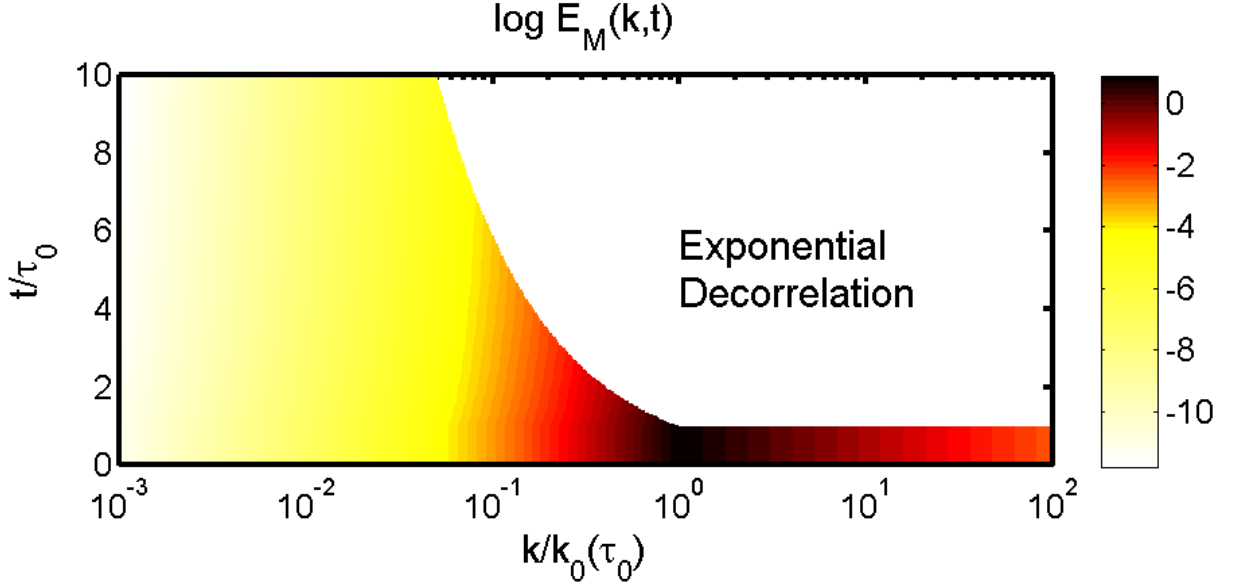


Figure 2. Spectral energy surface of the large-scale non-helical decaying turbulence $\log E_M(k, t)$. Free decay of turbulence starts at $t/\tau_0 = 1$. Exponential decorrelation occurs in the inertial region where $k > k_0$. In a $10\tau_0$ time period the spectral energy maximum drops by 5 orders of magnitude.

decay laws are strongly initial condition dependent, i.e. the free decay law depends on how the PMF was generated [7]; whether the PMF was generated through bubble collisions, leading to $l_0 \simeq v_b \beta^{-1}$ with v_b the bubble wall velocity and β the bubble nucleation rate parameter ($\beta \simeq 100 H_*$ for the EWPT) [24], or if the PMF was present prior to the PT [10]. Another uncertainty comes from the kinetic (vortical) energy density spectrum E_K [16].

The presence of even a small amount of magnetic helicity substantially affects PMF evolution [25, 26, 27, 28]. If there is only a little magnetic helicity, first a direct cascade develops. At the end of this first stage the turbulence relaxes to a maximally helical state [26, 27] that satisfies $|\mathcal{H}_M(t)| \leq 2\xi_M(t)\mathcal{E}_M(t)$ and the second inverse-cascade stage starts. Conservation of magnetic helicity implies that the magnetic energy density decays in inverse proportion to the correlation length growth during the inverse cascade. In contrast for the case of well-established non-helical turbulence, the effect of magnetic helicity is still under discussion [25, 26, 27, 28]. The main point of debate is related to the magnetic correlation length growth rate during the inverse cascade, i.e. $\xi_M(t) \propto t^{n_\xi}$, where the index n_ξ is argued to be $1/2$ [25, 26] or $2/3$ [27, 28]. The total magnetic energy density $\mathcal{E}_M(t) \propto t^{-n_\xi}$, and the decay of large-scale kinetic energy $\mathcal{E}_K(t)$ (and as a consequence the ratio between the magnetic and kinetic energy densities $\mathcal{E}_M(t)/\mathcal{E}_K(t)$) are sensitive to n_ξ . In particular, Refs. [25, 26] argue that $\mathcal{E}_K(t) \propto t^{-1}$, implying a faster decay of kinetic energy at large scales, while the results of Refs. [27, 28] lead to a constant $\mathcal{E}_M(t)/\mathcal{E}_K(t)$ within the inverse cascade and $\mathcal{E}_K(t) \propto t^{-2/3}$. In both these

models the magnetic turbulent energy density significantly decays on the phase transition timescale H_\star^{-1} , see Fig. 3.

3. Results and Discussion

The limits on the PMF at large scales are much stronger for the non-helical turbulence case; without the decay the constraint at zero redshift on 1 Mpc is 10^{-28} G for $\alpha = 4$ for an EWPT generated PMF, see Fig. 1 (also see Ref. [23]). In the $\alpha = 3/2$ case, the PMF can reach values of order $10^{-12} - 10^{-11}$ G that are required for seed MFs that might be able to explain observed MFs in galaxies and clusters [29]. Of course, large-scale decay of turbulence will strengthen these limits for both the non-helical and helical cases. On the other hand, accounting for large-scale PMF decay the BBN bound does not imply $\rho_B \leq 0.1\rho_{\text{rad}}$ when the PMF is generated. However, there is another requirement: the PMF cannot be the only component during the radiation dominated epoch, thus $\rho_B/\rho_{\text{rad}}(T_\star) < 1$. Even though our analysis is preliminary, it seems that a PT generated PMF requires an effective amplification mechanism (such as a dynamo), or a specific initial condition, to act as a viable seed field for observed MFs in galaxies and clusters. We will address this issue in future work [18].

A PT generated PMF may have observable cosmological signatures. In particular a PMF induces CMB anisotropies. Usually when considering PMF limits from CMB data one refers to the amplitude of the smoothed PMF, B_λ , on large scales $\lambda \sim 1$ Mpc [6]. On the other hand, when computing PMF induced CMB temperature and polarization anisotropy power spectra one finds $C_l \propto (B_\lambda^2 \lambda^{\alpha+1})^2$ [17, 30, 31], and when considering Faraday rotation of the CMB polarization plane the rotation angle and the resulting B-polarization power spectra are $\propto B_\lambda^2 \lambda^{\alpha+1}$ [5]. From the definition of B_λ above, it is clear that PMF imprints on CMB fluctuations are determined by Ω_B (or Ω_B^2), also see Refs. [32, 33].

On the other hand, the MF energy density evolves because of cosmological expansion, resulting in the time dependence of the damping wavenumber k_D . During a PT that generates the MF, or when the MF starts to interact with the plasma (if it had been generated prior to the PT), the total MF energy density at large scales is determined by the wavenumber of the peak of the MF spectral energy density, k_0 . The value of this peak is fixed by the maximal correlation length of the MF at the phase transition, and it is independent of future evolution and dissipation processes. In other word, during PTs all wavenumbers $k < k_0$ contribute to the total MF energy density. On the other hand, near the last scattering surface some modes have been damped and dissipated and thus the total energy density accounts for all wavenumbers $k < k_D$. k_D is not determined by MF dissipation by viscosity on small scales during the PT, but by other processes that occur during cosmological expansion. Note that $k_D \leq k_0$. Refs. [30, 32] study the damping of a homogeneous MF assuming the main dissipation process is Alfvén wave viscosity, resulting in $k_D^{-1} \simeq L_S v_A$, with L_S being the Silk damping scale at recombination and v_A determined by the background homogeneous PMF. For the case of a stochastic PMF, Ref. [31] defines v_A through the effective background MF, $B^{\text{eff}} = B_\lambda (\lambda/\lambda_D)^{(\alpha+1)/2}$, smoothed over the length scale $\lambda > \lambda_D$, so k_D becomes B_λ , λ , and α dependent. Such a description appears inconsistent with the picture of Alfvén wave induced dissipation,

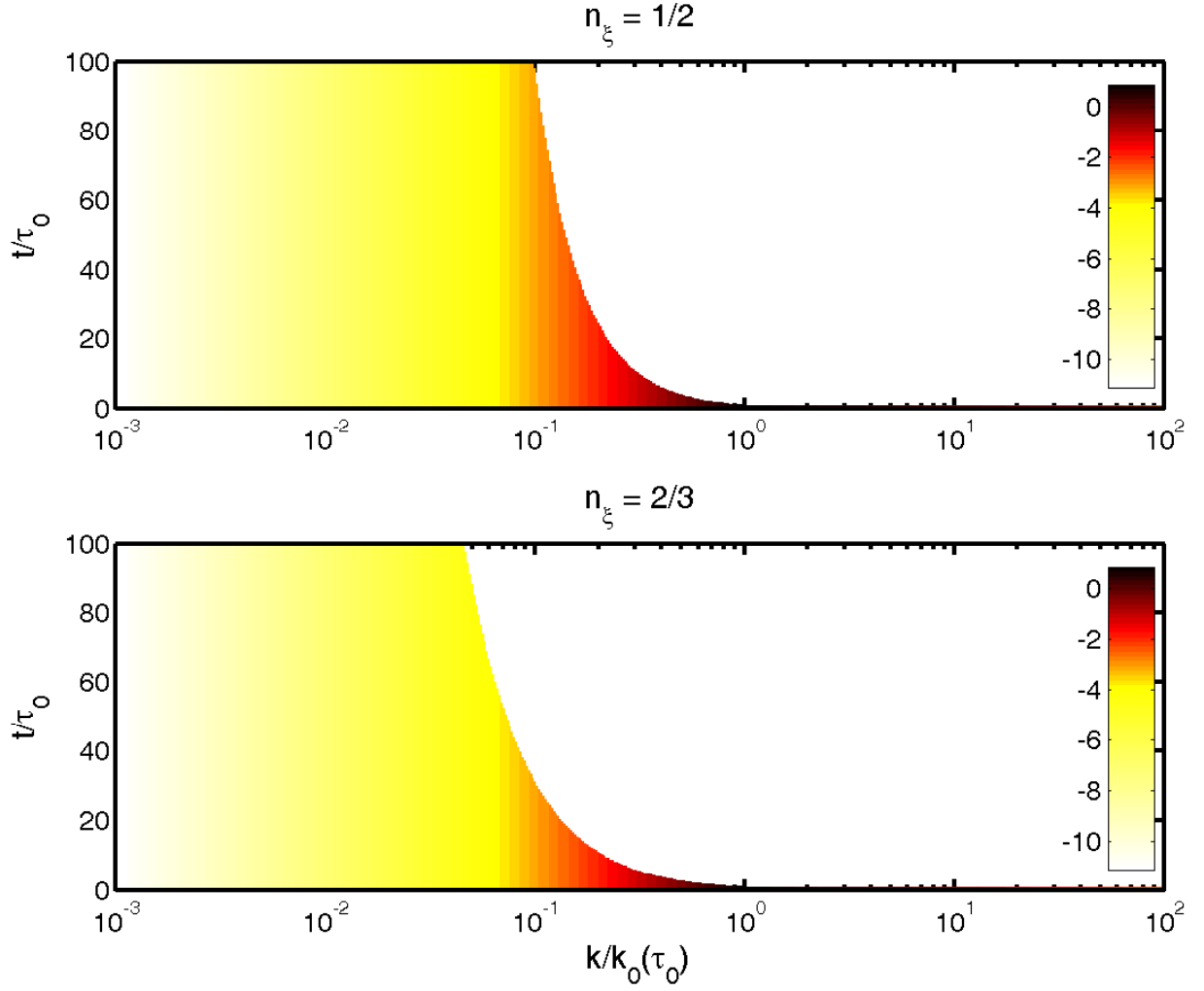


Figure 3. Spectral energy surfaces of the large-scale helical turbulence $\log E_M(k, t)$. The upper and lower panels correspond to the $n_\xi = 1/2$ and $n_\xi = 2/3$ decay laws, respectively. In a $100\tau_0$ time period the maximal spectral energy drops by 3 and 5 orders of magnitude in the two cases, respectively.

since the effective background field when $\alpha \geq 0$ is significantly smaller than that associated with the fluctuating Alfvén wave MF. As a result the damping scale $k_D \ll k_0$ and only a small part of the initial MF energy contributes to the CMB anisotropies. Accounting for this, a PMF with $\alpha = 4$ and amplitude of order 10^{-13} G at 1 Mpc contributes to CMB fluctuations, while a scale-invariant PMF with $\alpha \simeq -1$ and amplitude larger than 10^{-9} G might leave observable CMB anisotropy traces. On the other hand, ignoring Alfvén wave induced damping (and not determining v_A through the amplitude of the PMF at scales corresponding to L_S) we can conclude that even if EWPT or QCDPT generated PMFs have a small amplitude at large scales, if 1 – 10% of the radiation energy density is in the form of a PMF, the observable CMB anisotropy consequences will be similar to those of an inflation-generated PMF with $10^{-9} - 10^{-10}$ G now at 1 Mpc.

Another interesting effect is relic gravitational wave (GW) generation [8, 9, 34]. The amplitude of these GWs is determined by the amount of MF energy density present at the PT, and it is not influenced by further MF damping. Direct cascade MHD turbulence generates GW with amplitude

$$h_C(f) \simeq 1.2 \times 10^{-15} v_A \gamma^{5/2} \left(\frac{100 \text{ GeV}}{T_*} \right) \left(\frac{100}{g_*} \right)^{1/3} \left(\frac{f}{f_H} \right)^{1/2} S^{1/2}(f), \quad (3)$$

where f is the frequency now, $f_H = \lambda_H^{-1} \simeq 1.6 \times 10^{-5} \text{ Hz} (g_*/100)^{1/6} (T_*/100 \text{ GeV})$ is the Hubble frequency now, and $S(f)$ is determined by the MF statistical properties,

$$S(f) = C_M^2 \int_1^{\text{Re}^{3/4}} \frac{dx}{x^6} \exp\left(-\frac{f^2 \gamma^2}{f_H^2 v_A^2 x^{4/3}}\right) \text{erfc}\left(-\frac{f \gamma}{f_H v_A x^{2/3}}\right), \quad (4)$$

where $\text{erfc}(x)$ is the complementary error function defined as $\text{erfc}(x) = 1 - \text{erf}(x)$, where $\text{erf}(x) = \int_0^x dy \exp(-y^2)$ is the error function. As expected, the integral in Eq. (4) is dominated by the large scale ($x \simeq 1$) contribution.

The amplitude and the energy density of the GW are related through,

$$h_C(f) = 1.26 \times 10^{-18} \left(\frac{\text{Hz}}{f} \right) [h_0^2 \Omega_{\text{GW}}(f)]^{1/2}, \quad (5)$$

where $\Omega_{\text{GW}}(f)$ is the GW spectral energy density parameter. Using Eqs. (3) and (5), we have

$$\Omega_{\text{GW}}(f) h_0^2 = 2.3 \times 10^{-4} v_A^2 \gamma^5 \left(\frac{100}{g_*} \right)^{1/3} \left(\frac{f}{f_H} \right)^3 S(f). \quad (6)$$

Integrating $\Omega_{\text{GW}}(f)$ over frequency, it can be seen that the efficiency of GW production is low, $\propto v_A^3 \gamma^2$, with peak GW frequency for the EWPT being $f_{\text{peak}} \simeq \gamma^{-1} v_A \lambda_H^{-1}$ [35] (and an additional peak at λ_H^{-1} for helical MHD turbulence [36]), but the signal is potentially observable by LISA [34]. For lower frequencies $f \ll f_H$, $\Omega_{\text{GW}} \propto f^3$, and for high frequencies $f \gg f_H$ there is exponential damping. The peak amplitude of $\Omega_{\text{GW}}(f_{\text{peak}}) = 2.3 \times 10^{-4} v_A^5 \gamma^2 (g_*/100)^{-1/3}$ and is independent of T_* . The analysis above shows that the main contribution to the GW background comes from the EWPT and we can ignore the expansion of the Universe when studying GW generation (even for a helical PMF).

4. Conclusion

We have constrained a causally generated PMF produced prior to BBN, by using the BBN bound on the relativistic energy density during nucleosynthesis. We can also constrain a PMF generated after nucleosynthesis, but still during the radiation-dominated epoch, by requiring that the PMF energy density not be the dominant component. Figure 1 shows the PMF limits without accounting for damping or decay of the PMF. This is because PMF large-scale decay is very model dependent, and to study this case requires accounting for the initial conditions.

We have also argued that directly using the smoothed PMF, B_λ , might cause confusion. We instead propose using the PMF energy density when deriving constraints from PMF cosmological signatures. In particular, using $\xi_m(t) \propto t^{n_\xi}$ (where the correlation length is associated with the largest size MF eddy $\lambda_0 = 2\pi/k_0$) together with $\mathcal{E}_M \propto t^{-n_E}$, in the framework of $\mathcal{E}_M^{\text{LS}} \propto B_\lambda^2(\lambda k_0)^{\alpha+1}$, implies that $B_\lambda(t) \propto t^{((\alpha+1)n_\xi - n_E)/2}$, leading to B_λ increasing if the smoothing scale λ is fixed, while the real MF energy density is decreasing. It is obvious that B_λ increasing in time is not a physical effect. Another advantage of using the PMF energy density is the independence of the BBN limit on the energy scale when the generation occurs (T_\star), even though all characteristic length scales are strongly T_\star dependent.

Free turbulence decay on large scales (even without knowing the exact scaling law) allows us to conclude that after the PT ends turbulence has been largely damped, and there is no available source to produce the gravitational radiation at the same level as that from the PT itself. This allows us to neglect cosmological expansion when considering the GW generation process. Accounting for this, the direct detection of relic GWs will allow us to study the PT MHD turbulence picture, if enough (1-10%) of the thermal energy during the PT is present in the form of MF energy density.

We appreciate helpful comments from A. Brandenburg and K. Jedamzik and acknowledge useful discussions with C. Caprini, R. Durrer, S. Huber, L. Kisslinger, A. Kosowsky, T. Stevens, K. Subramanian, and T. Vachaspati. We acknowledge partial support from GNSF grants Pres-07/153 and ST08/4-442 and DOE grant DE-FG03-99EP41043. T.K. acknowledges the ICTP associate membership program, and NORDITA for hospitality during the Electroweak Phase Transitions workshop.

REFERENCES

1. L. M. Widrow, Rev. Mod. Phys. 74 (2002) 775 .
2. J. P. Vallée, New Astron. Rev. 48 (2004) 763.
3. B. Ratra and M. S. Vogeley, Publ. Astron. Soc. Pac. **120**, 235 (2008).
4. A. Kosowsky and A. Loeb, Astrophys. J. 469 (1996) 1; M. Giovannini, Phys. Rev. D 56 (1997) 3198; T. Kolatt, Astrophys. J. 485 (1998) 564; S. Sethi, Mon. Not. Astron. Soc. 342 (2003) 962; L. Campanelli, A.D. Dolgov, M. Giannotti and F.L. Villante, Astrophys. J. 616 (2004) 1; M. Giovannini, Phys. Rev. D 71 (2005) 021301; F. Finelli and M. Galaverni, Phys. Rev. D 79 (2009) 063002; M. Giovannini and K. E. Kunze, arXiv:0804.2238 [astro-ph], Phys. Rev. D 78 (2008) 023010.
5. A. Kosowsky, T. Kahniashvili, G. Lavrelashvili, and B. Ratra, Phys. Rev. D 71 (2005)

- 043006; T. Kahniashvili, Y. Maravin, and A. Kosowsky, Phys. Rev. D 80 (2008) 023009.
6. M. Giovannini, Class. Quant. Grav. 23 (2006) R1.
 7. E. R. Harrison, Mon. R. Astron. Soc 147 (1970) 279; T. Vachaspati, Phys. Lett. B 265 (1991) 258; A. Brandenburg, K. Enqvist, and P. Olesen, Phys. Rev. D 54 (1996) 1291; J. M. Cornwall, Phys. Rev. 56 (1997) 6146; G. Sigl, A. V. Olinto, and K. Jedamzik, Phys. Rev. D 55 (1997) 4582; M. Joyce and M. E. Shaposhnikov, Phys. Rev. Lett. 79 (1997) 1193; M. Hindmarsh and A. Everett, Phys. Rev. C 58 (1998) 103505; K. Enqvist, Int. J. Mod. Phys. D 7 (1998) 331; J. Ahonen and K. Enqvist, Phys. Rev. D 57 (1998) 664; M. Giovannini, Phys. Rev. D 61 (2000) 063004; T. Vachaspati, Phys. Rev. Lett. 87 (2001) 251302; A. D. Dolgov and D. Grasso, Phys. Rev. Lett. 88 (2002) 011301; D. Grasso and A. Dolgov, Nucl. Phys. Proc. Suppl. 110 (2002) 189; D. Boyanovsky, M. Simionato, and H. J. de Vega, Phys. Rev. D 67 (2003) 023502; D. Boyanovsky, H. J. de Vega, and M. Simionato, Phys. Rev. D 67 (2003) 123505; M. B. Johnson, L. S. Kisslinger, E. M. Henley, W.-Y.P. Hwang, and T. Stevens, Mod. Phys. Lett. A 19 (2004) 1187; L. Campanelli and M. Giannotti, Phys. Rev. D 72 (2005) 123001; A. Diaz-Gil, J. Garcia-Bellido, M. Garcia Perez, and A. Gonzalez-Arroyo, Phys. Rev. Lett. 100 (2008) 241301; T. Stevens and M. B. Johnson, arXiv:0903.2227[astro-ph].
 8. D. V. Deriagin, D. Iu. Grigor'ev, V. A. Rubakov, and M. V. Sazhin, Mon. Not. R. Astron. Soc. 229 (1987) 357.
 9. C. Caprini and R. Durrer, Phys. Rev. D 65 (2001) 023517.
 10. B. Ratra, Astrophys. J. 391 (1992) L1; K. Bamba, N. Ohta, and S. Tsujikawa, Phys. Rev. D 78 (2008) 043524.
 11. e.g., J. Cornwall, Phys. Rev. D 56 (1997) 6146; M. Giovannini and M. E. Shaposhnikov, Phys. Rev. D 57 (1998) 2186; G. B. Field and S. M. Carroll, Phys. Rev. D 62 (2000) 103008; T. Vachaspati, Phys. Rev. Lett. 87 (2001) 251302; L. Campanelli and M. Giannotti, Phys. Rev. D 72 (2005) 123001; A. Diaz-Gil, J. Garcia-Bellido, M. Garcia Perez and A. Gonzalez-Arroyo, Phys. Rev. Lett. 100 (2008) 241301; L. Campanelli, arXiv:0805.0575 [astro-ph].
 12. D. Biskamp, *Magnetohydrodynamic Turbulence* (Cambridge University, Cambridge, 2003); M. K. Verma, Phys. Rept. 401 (2004) 229.
 13. C. J. Hogan, Phys. Rev. Lett. 51 (1983) 1488.
 14. R. Durrer and C. Caprini, JCAP 0311 (2003) 010.
 15. P. A. Davidson, *Turbulence* (Oxford University, Oxford, 2004).
 16. M. Christensson, M. Hindmarsh, and A. Brandenburg, Phys. Rev. E 70 (2001) 056405; N. E. Haugen, A. Brandenburg, and W. Dobler, Phys. Rev. E 70 (2004) 016308.
 17. T. Kahniashvili and B. Ratra, Phys. Rev. D 75 (2007) 023002.
 18. T. Kahniashvili, A. Brandenburg, A. G. Tevzadze, and B. Ratra, (in preparation).
 19. I. Proudman, Proc. R. Soc. London A 214 (1952) 119; A. S. Monin and A. M. Yaglom, *Statistical Fluid Mechanics* (MIT Press, Cambridge, MA, 1975).
 20. A. Kosowsky, A. Mack, and T. Kahniashvili, Phys. Rev. D 66 (2002) 024030.
 21. R. H. Kraichnan, Phys. Fluids 7 (1964) 1163.
 22. B. P. Pope, *Turbulent Flows* (Cambridge University, Cambridge, 2000).
 23. C. Caprini, R. Durrer, and E. Fenu, arXiv:0906.4976 [astro-ph.CO].

- 24. T. Kahniashvili, L. Kisslinger, and T. Stevens, arXiv:0905.0643 [astro-ph.CO].
- 25. D. Biskamp and W.-C. Müller, Phys. Rev. Lett. 83 (1999) 2195; Phys. Plasma 7 (2000) 4889; D. T. Son, Phys. Rev. D 59 (1999) 063008.
- 26. M. Christensson, M. Hindmarsh, and A. Brandenburg, Astron. Nachrichten 326 (2005) 393.
- 27. R. Banerjee and K. Jedamzik, Phys. Rev. Lett. 91 (2003) 251301; Phys. Rev. D 70 (2004) 123003.
- 28. L. Campanelli, Phys. Rev. Lett. 98 (2007) 251302.
- 29. K. Dolag, M. Bartelmann, and H. Lesch, Astron. Astrophys. 387 (2002) 383.
- 30. K. Subramanian and J. D. Barrow, Phys. Rev. Lett. 81 (1998) 3575; Phys. Rev. D 58 (1998) 083502.
- 31. A. Mack, T. Kahniashvili, and A. Kosowsky, Phys. Rev. D 65 (2002) 123004; D. G. Yamazaki, K. Ichiki, K. Toshitaka, and G. J. Mathews, Mod. Phys. Lett. A 23 (2008) 1695; D. G. Yamazaki, K. Ichiki, T. Kajino, and G. J. Mathews, Phys. Rev. D 77 (2008) 043005; Phys. Rev. D 78 (2008) 123001.
- 32. K. Jedamzik, V. Katalinic, and A. V. Olinto, Phys. Rev. Lett. 85 (2000) 700.
- 33. T. R. Seshadri and K. Subramanian, arXiv:0902.4066 [astro-ph.CO].
- 34. T. Kahniashvili, L. Campanelli, G. Gogoberidze, Y. Maravin, and B. Ratra, Phys. Rev. D 78 (2008) 123006.
- 35. G. Gogoberidze, T. Kahniashvili, and A. Kosowsky, Phys. Rev. D 76 (2007) 083002.
- 36. T. Kahniashvili, G. Gogoberidze, and B. Ratra, Phys. Rev. Lett. 100 (2008) 231301.